Road Materials and Pavement Design

ISSN: 1468-0629 (Print) 2164-7402 (Online) Journal homepage: https://www.tandfonline.com/loi/trmp20

# Using the GMDH and ANFIS methods for predicting the crack resistance of fibre reinforced high RAP asphalt mixtures

Hassan Ziari, Amir Amini, Ali Moniri & Mahdi Habibpour

**To cite this article:** Hassan Ziari, Amir Amini, Ali Moniri & Mahdi Habibpour (2020): Using the GMDH and ANFIS methods for predicting the crack resistance of fibre reinforced high RAP asphalt mixtures, Road Materials and Pavement Design, DOI: 10.1080/14680629.2020.1748693

**To link to this article:** https://doi.org/10.1080/14680629.2020.1748693

Published online: 08 Apr 2020.

ROAD MATERIALS AND PAVEMENT DESIGN
https://doi.org/10.1080/14680629.2020.1748693



# Using the GMDH and ANFIS methods for predicting the crack resistance of fibre reinforced high RAP asphalt mixtures

Hassan Ziari[a], Amir Amini[b], Ali Moniri [b] and Mahdi Habibpour[b]

[a]Asphalt and Bitumen Research Center (ABRC), School of Civil Engineering, Iran University of Science and Technology (IUST), Narmak, Tehran, Iran; [b]School of Civil Engineering, Iran University of Science and Technology (IUST), Narmak, Tehran, Iran

**ABSTRACT**

In this paper, the effectiveness of the group method of data handling (GMDH) and the adaptive neuro-fuzzy inference system (ANFIS) methods in modelling the fracture parameters of asphalt mixtures were studied. For this aim, the models were investigated on the fracture energy and J-integral results of hot mix asphalt in terms of temperature, RAP content and fibre content. It was found that the fibres have an outstanding effect on the fracture behaviour of asphalt mixtures especially at intermediate and high temperatures and can be considered as an alternative to enhance the fracture resistance of recycled asphalt mixtures. The fracture data of asphalt mixtures can be successfully modelled by the ANFIS method with a high level of correlation. The GMDH was unable to model the J-integral results, however, it had a fair correlation with the results of fracture energy.

**ARTICLE HISTORY**
Received 1 October 2019
Accepted 17 March 2020

**KEYWORDS**
group method of data handling (GMDH); adaptive neuro-fuzzy inference system (ANFIS); SCB fracture test; reclaimed asphalt pavement; Fiber-reinforced asphalt

## 1. Introduction

Low temperature cracking, fatigue and rutting are of the most occurrence distresses of asphalt mixtures (Korayem et al., 2018; Sabouri et al., 2018; Ziari et al., 2016b, 2016d). Low-temperature cracking is the most prevalent defect in areas with harsh cold weather and high temperature gradient (Aliha et al., 2014, 2015; Aliha & Sarbijan, 2016). There are numerous methods for measuring the resistance of asphalt mixtures against low-temperature cracking, from which using fracture mechanics is known as one of the most reliable techniques (Aliha et al., 2016; Ameri et al., 2016; Haghighat Pour et al., 2018; Saha & Biligiri, 2016). Many researchers have used the fracture mechanic approach for investigating the cracking behaviour of asphalt mixtures (Aliha et al., 2017; Behbahani et al., 2013; Fattahi Amirdehi et al., 2019). Fracture toughness, fracture energy and J integral are of the most common fracture parameters used to describe the cracking behaviour of asphalt mixtures (Ling et al., 2019; Mohammad et al., 2012; Saha & Biligiri, 2016). As fracture toughness is defined as a fracture resistance parameter for elastic material, it can only be used at minus temperatures for asphalt mixtures, at which the performance of asphaltic material is linear elastic. However, fracture energy and J integral can be used to investigate the cracking resistance of asphalt specimens at all temperatures (Aliha, 2019; Ameri et al., 2016; Haghighat Pour et al., 2018; Minhajuddin et al., 2015).

Previous researches have shown that using high contents of reclaimed asphalt pavement (RAP) material in asphalt mixtures weakens the cracking behaviour of the mixtures. As the cracking resistance declines by increasing the brittleness of material, using RAP materials that contain aged brittle bitumen can lead to a decrease in cracking resistance of asphalt mixtures (et al., 2019; Jing et al., 2019;

**CONTACT** Hassan Ziari h.ziari@iust.ac.ir

Mansourkhaki et al., 2019b, 2020a; Sirin et al., 2018). On the other hand, the lack of natural resources such as aggregate and bitumen has inspired the researchers to use high contents of RAP material in asphalt mixtures (Ayazi et al., 2017; Behbahani et al., 2017; Mansourkhaki et al., 2020b; Ziari et al., 2017). For this purpose, different types of rejuvenators are introduced to the industry to restore the properties of the aged bitumen of RAP material (Ameri et al., 2019; Mansourkhaki et al., 2019a; Moghaddam & Baaj, 2016; Moniri et al., 2019; Zaumanis & Mallick, 2015; Zhou et al., 2019; Ziari et al., 2019b). However, the performance of the mixtures containing 100% rejuvenated RAP material is still questionable. Therefore, a complementary technique to compensate for the reduction in cracking resistance of the 100% RAP mixtures is required (Zaumanis et al., 2015).

In this regard, using polymer-modified virgin binders was reported to be effective in improving the cracking behaviour of the RAP mixtures. Previous studies showed that Styrene–butadiene–styrene (SBS) and styrene–butadiene rubber (SBR) latex modified virgin binder could enhance the fatigue and cracking performance of the recycled mixtures containing up to 50% of RAP material (Kodippily et al., 2017; Zhou et al., 2016). Using crumb rubber as a virgin bitumen modifier is also efficient in improving the fatigue and cracking behaviour of recycled asphalt mixtures (Ding et al., 2019). However, by increasing the RAP content, the amount of the virgin bitumen decreased and using polymer modified virgin binders cannot help the cracking behaviour of the mixtures. Therefore, additives such as fibres that are added directly to the mixtures can be an appropriate alternative to make up the negative resistance of RAP material on fatigue and cracking performance of the mixtures (Abtahi et al., 2010; Dehghan & Modarres, 2017; Mansourian et al., 2016; McDaniel, 2015; Park et al., 2015; Qin et al., 2018; Slebi-Acevedo et al., 2019; Ziari et al., 2020, 2019c). Glass fibres, which are categorised as high strength fibres, are reported to be effective in increasing the healing capability, rutting, fatigue and cracking resistance of asphalt mixtures (Enieb et al., 2019; Khanghahi & Tortum, 2018; Morea & Zerbino, 2018; Najd et al., 2005; Ziari & Moniri, 2019). In this study, different percentages of glass fibres were used in hot mix asphalt (HMA) containing different percentages of RAP material, and the cracking behaviour of the mixtures was evaluated using fracture mechanic techniques.

Evaluating and predicting the behaviour of modified asphalt mixtures often has problems such as time spent and high laboratory costs. In recent years, pioneering researchers have been looking for alternatives with high reliability and low cost to predict the behaviour of material (Sharifi et al., 2020; Ziari et al., 2018). Therefore, developing numerical models such as analytical neural network (ANN), adaptive network-based fuzzy inference system (ANFIS), group method of data handling (GMDH) and etc. can help future researchers to eliminate costly experiments. Ziari et al. in (2016) investigated the accuracy of the ANFIS and GMDH models for predicting the short and long term performance of asphalt pavements. They showed that the ANFIS method was more accurate than the GMDH model (Ziari et al., 2016a). The GMDH algorithm was successfully employed for modelling the moisture resistance of asphalt mixtures made with nano-silica modified bitumen (Sezavar et al., 2019). The ANFIS model was also used as a successful approach to predict different characteristics of asphaltic material (Moghaddam et al., 2015; Pourtahmasb et al., 2015; Tabatabaei et al., 2013). It can be seen in the previous researches that the significance of the prediction model differs for different mixes, and depending on the studied subject, different models should be used. On the other hand, little literature exists about numerical modelling of the fiber-reinforced recycled asphalt mixtures. Therefore, in this research, the GMDH and the ANFIS methods were investigated to model the fracture energy until failure, total fracture energy and the J integral of asphalt mixtures containing different percentages of RAP and glass fibres.

## 2. Materials

### 2.1. Bitumen

A PG 64-16 bitumen provided from Pasargad oil company was used as virgin bitumen to provide the specimens. The physical properties of the virgin bitumen are summarised in Table 1.

**Table 1.** Physical properties of asphalt binder.

| Test | Unit | Standard | PG 64–16 |
|---|---|---|---|
| Viscosity Test at 135°C (cSt) | centistokes | ASTM D113 | 364 |
| Penetration Test (0.1 mm) | 0.1 mm | ASTM D5 | 66 |
| Ductility Test (cm) | cm | ASTM D113 | 100 |
| Softening point (°C) | °C | ASTM D36 | 49 |
| Flash point (°C) | °C | ASTM D92 | 290 |
| Specific Gravity | g/cm$^3$ | ASTM D70 | 1.018 |

**Table 2.** Physical properties of the limestone aggregates used in this research.

| Test | Unit | Standard | Result |
|---|---|---|---|
| Coarse aggregate specific gravity | g/cm$^3$ | ASTM C127 | 2.57 |
| Fine aggregate specific gravity | g/cm$^3$ | ASTM C128 | 2.54 |
| Los Angeles abrasion value (LAV) | % | ASTM C131 | 22.2 |
| Sodium sulfate soundness (SS) | % | ASTM C88 | 2.7 |
| Sand equivalent (SE) | % | ASTM T176 | 65 |
| Flakiness | % | BS-812 | 16.63 |

**Table 3.** Properties of the glass fibres used in this research.

| Feature | Unit | Glass fibre |
|---|---|---|
| Color | – | White |
| Specific gravity | g/cm$^3$ | 1.18 |
| Length | mm | 12 |
| Diameter | mm | $< 0.13$ |
| Tensile strength | MPa | $> 1000$ |
| Melting point | °C | 800–900 |
| Water absorption | % | 0 |

## 2.2. Aggregates

Limestone aggregates obtained from quarries, which are usually used for asphalt production, were used as virgin aggregates in this study. The physical characteristics of the aggregates used in this research are presented in Table 2.

## 2.3. Fibres

In this study, high strength glass fibres which consist of numerous glass wools were used for reinforcing the recycled mixtures. The fibres were produced exclusively to be used in asphalt mixtures. Therefore, they have a high melting point. The characteristics of this fibre are listed in Table 3. An example image of these fibres is shown in Figure 1.

## 2.4. Rejuvenator

Cyclogen, which is categorised as aromatic extract oils, was used as rejuvenator of RAP material. The function of rejuvenator is to diffuse into the aged bitumen and modify its characteristics. Therefore, the optimum dosage of these materials can be found by testing its effect on the performance grade of the recovered RAP bitumen (Naderi et al., 2019; Zaumanis et al., 2014; Ziari et al., 2019a). Therefore, different percentages of the rejuvenator added to the RAP bitumen, recovered according to AASHTO TP 2, and the optimum dose of the rejuvenator was selected as 6% of total RAP bitumen by testing the performance grade of the specimens.

Colour online, B/W in print

**Figure 1.** Glass fibre used in this research.

**Table 4.** The gradation of the RAP material used in this research.

| | | | | | | |
|---|---|---|---|---|---|---|
| Sieve Size (mm) | 19 | 12.5 | 4.75 | 2.36 | 0.3 | 0.075 |
| Results | 100 | 98.2 | 69.3 | 47.2 | 15.8 | 6 |

### 2.5. RAP material

The RAP material was obtained from the milling operation of a highway in Tehran. Different samples from different sections of the RAP stockpile were taken and the average bitumen content of the RAP material was determined as 5.4%. The average gradation of the extracted aggregates of the RAP material is also presented in Table 4.

## 3. Methodology

### 3.1. Mix design

The Marshall mix design procedure was employed to determine the mix design and volumetric properties of the mixtures containing 0%, 25%, 50%, 75%, and 100% RAP material based on AASHTO T245 (2004). It was found that the required virgin binder content substantially decreases by increasing the RAP content in the mixtures. A slight decrease in the specific gravity was also resulted by increasing the percentage of the RAP material. This was mainly due to the layered bitumen structure in the RAP material. In other words, some proportion of the aged bitumen of the RAP material does not participate in the remixing process and stick to the RAP aggregates, which are called black aggregates. These aggregates have less specific gravity than the virgin aggregates. A summary of the mix design is shown in Table 5.

### 3.2. Sample preparation

For preparing the samples, at first, the virgin aggregates and RAP material were placed at mixing temperature of 175°C for 16 and 2 h respectively. The RAP material was then mixed with the rejuvenator and added to the aggregates and stirred. The fibres were gradually added to the mix during stirring.

**Table 5.** Summary of mix design.

| Parameter | 0% RAP | 25% RAP | 50% RAP | 75% RAP | 100% RAP |
|---|---|---|---|---|---|
| Optimum virgin binder (% of total mix) | 5.4 | 3.93 | 2.55 | 1.23 | 0.25 |
| Marshall Stability(KN) | 8.2 | 8.4 | 10.9 | 16.1 | 17.6 |
| Bulk density (gr/cm3) | 2.37 | 2.36 | 2.35 | 2.33 | 2.32 |

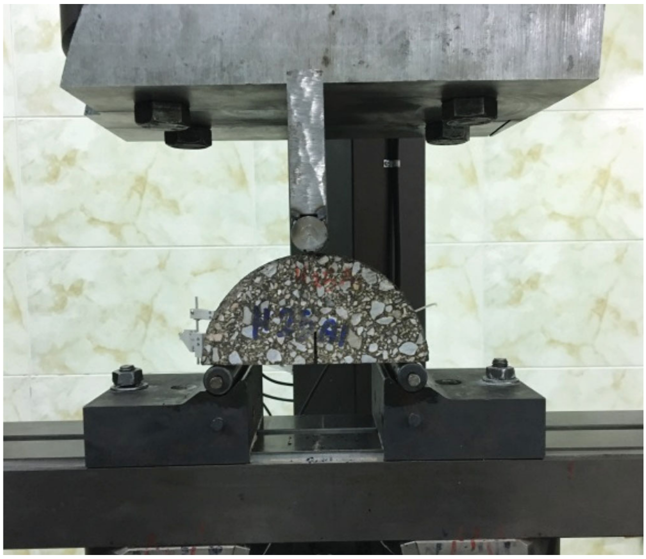



**Figure 2.** The fixture of the SCB fracture test.

The virgin bitumen was then added to the mix. Finally, the total mixtures were kept in compaction temperature for two hours (Haghshenas et al., 2016). The compaction procedure was conducted using the Superpave gyratory compactor (SGC) with a 150 mm diameter mould. The mixtures were compacted until reaching the target air void, which was calculated using the volumetric properties of the mixtures obtained from mix design (Korayem et al., 2018; Sabouri et al., 2018; Ziari et al., 2016b, 2017). For each mixture, three SGC specimens were manufactured. Each compacted cylindrical specimens were then cut to four SCB specimens with a thickness of 57 mm. A notch with 0.3 mm width and lengths of 25, 32 and 38 mm were then created in the middle of SCB specimens.

### 3.3. SCB fracture tests

The mode I fracture tests were conducted on the SCB specimens using a tension-compression testing machine with a loading capacity of 50 kN. The distance of the supports was chosen as 127 mm as shown in Figure 2. The test was carried out at temperatures of −15, 0 and 15 °C by applying a linear load with a rate of 0.5 mm/min. Four replicates were conducted for each notch depth. The failure criteria were chosen as the fracture energy before failure, the total fracture energy and the critical value of J integral. The fracture energy until failure is calculated as the area under the load-displacement curve before the peak load, which shows the resistance of a material against crack initiation. The total fracture energy, which is a criterion of crack propagation, is calculated as the total area under the load-displacement curve (Minhajuddin et al., 2015; Saha & Biligiri, 2015). The fracture energy until failure and the total fracture energy were calculated for the specimens with a 25 mm notch length for the sake of brevity.

Another criterion used in this study to determine the crack resistance of the mixtures was the critical value of J-integral (Jc). This parameter is reported to be a promising method for evaluating the cracking performance of asphalt mixtures (Jahanbakhsh et al., 2019; Ling et al., 2019; Luo et al., 2016; Song et al., 2018). Equation 1 was used to calculate the critical value of J integral. In this equation, U is the fracture energy, a is the notch length and b is the thickness of the specimens. The notch depth values were 25, 32 and 38 mm in this research.

$$\mathrm{J}_c = -\frac{1}{b}\frac{dU}{da} \tag{1}$$

### 3.4. Prediction models

In this research, the fracture energy until failure, total fracture energy, and the Jc value were modelled in terms of the RAP content, fibre content and testing temperature using the ANFIS and the GMDH methods, which are described as follows:

#### 3.4.1. The GMDH method

The GMDH is a multivariate analysis approach for modelling complex functions with numerous variables, which was firstly proposed by Ivakhnenko in 1966 (Ivakhnenko, 1971). The GMDH is a prediction model that works based on regression-based algorithms by using a class of polynomials from independent variables to investigate the interactions among the variables (Ziari et al., 2016a). The basic GMDH model is shown in Equation 2. This model relates the variables to an output by constructing a class of polynomials (Ziari et al., 2016c).

$$Y = a + \sum_{i=1}^{m} b_i x_i + \sum_{i=1}^{m}\sum_{j=1}^{m} c_{ij} x_i x_j + \sum_{i=1}^{m}\sum_{j=1}^{m}\sum_{k=1}^{m} d_{ijk} x_i x_j x_k + \sum_{i=1}^{m}\sum_{j=1}^{m}\sum_{k=1}^{m}\sum_{l=1}^{m} e_{ijkl} x_i x_j x_k x_l + \cdots \quad (2)$$

Where m is the number of input variables, x is the input variable, y is the model output and a, bi, cij, dijk, eijkl, etc. are the coefficients of the model.

#### 3.4.2. The ANFIS method

The ANFIS method is defined as a kind of artificial neural network that is functionally equivalent to the fuzzy inference systems. This approach integrates both ANN and fuzzy logic prinsiples, and has the advantages of both methods (Abraham, 2005). The ANFIS system improves the accuracy of the predicted results by determining the fuzzy interference system indexes using ANN algorithms (Mohandes et al., 2011). In the ANFIS system, the structure of the model is firstly introduced based on the membership functions of the input and output variables and the rules of the network learning. At the training stage, the output of the nodes of all layers is calculated, and then the result indicators are calculated using the least-squares sum error method. Afterwards, the error ratios are distributed on conditional indices and their values are corrected using the descending slope error method (Kim et al., 2013). After training the data and determining the model parameters, the accuracy of the ANFIS model should be validated in order to predict the output values of the corresponding input data. A simplified schematic framework of the ANFIS model is illustrated in Figure 3. It can be seen in this Fig that the ANFIS model is composed of 5 layers. In layer 1, Every node is an adaptive node with node function expressed as shown in equations 3 and 4. In layer 2 every node becomes a fixed node. In this layer, the node function should be multiplied by the input signals to serve as the output signals, which represent the firing strength of

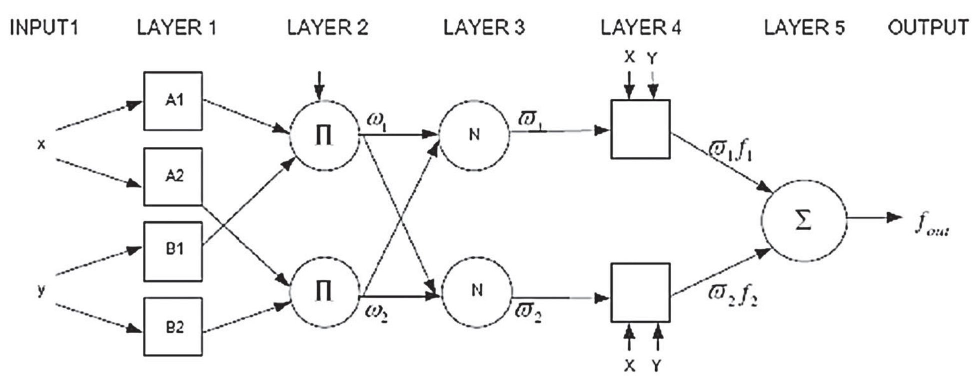


**Figure 3.** The schematic frame work of the ANFIS model.

a rule. This layer is shown in equation 5. In layer 3, the ratio of the $i_{th}$ output to the sum of all outputs is calculated to normalise the node output as shown in equation 6. In layer 4, the normalised output is multiplied by the fuzzy if–then rules which are presented in equations 7. Finally, the overall output is computed in the fifth layer using equation 8.

$$O_{1.i} = \mu_{A_i}(x) \quad \text{for } i = 1, 2, \tag{3}$$

$$O_{1.i} = \mu_{B_i}(y) \quad \text{for } i = 3, 4, \tag{4}$$

$$O_{2.i} = \mu_{A_i}(x) \times \mu_{B_i}(y) = W_i \quad \text{for } i = 1, 2 \tag{5}$$

$$O_{3.i} = \frac{W_i}{\sum W_i}\, i = 1, 2 \tag{6}$$

$$O_{4.i} = \bar{W}_i \times f_i\, i = 1, 2 \tag{7}$$

$$O_{5,i} = \sum_i \bar{W}_i \times f_i = \frac{\sum_i W_i f}{\sum_i W_i} \tag{8}$$

The most important shortcoming of the ANFIS system is its failure in determining the network parameters such as the number and type of membership functions of the input and output variables and the optimal network learning parameters (Pourtahmasb et al., 2015). Therefore, in this research, various ANFIS structures are investigated based on the number and type of membership functions in order to determine the best structure for modelling. The inputs of the fuzzy inference system in this study are fibre content, RAP content and temperature, and the outputs fracture energy until failure, total fracture energy and the Jc value. The training and testing of the fuzzy system were conducted using the Fuzzy logic option in the MATLAB software.

### *3.4.3. Statistical analysis*

In this research, the damped least-squares method was utilised to minimise the error of the model using the MATLAB software. For this purpose, 60% of experimental data were used for training, 20% for cross-validation and 20% for test data. The significance of the trained networks was also investigated using the Squared Correlation Coefficient ($R^2$), Root Mean Square Error (RMSE), and Coefficient of Variation (COV) parameters (Kök et al., 2013), which were calculated using equations 9–11 respectively.

$$\mathrm{RMSE} = \sqrt{\frac{\sum_{i=1}^{n} (Y^{pre} - Y^{mea})^2}{n}} \tag{9}$$

$$R^2 = 1 - \frac{\sum_{i=1}^{n} (Y^{mea} - Y^{pre})2}{\sum_{i=1}^{n} (Y^{mea} - \bar{Y})^2} \tag{10}$$

$$\mathrm{COV} = \frac{\mathrm{RMSE}}{|\bar{Y}^{mea}|} \times 100 \tag{11}$$

Where $Y^{mea}$ is the observed value, $Y^{pre}$ is the estimated value and $\bar{Y}$ is the average of observed values.

The analysis of variance (ANOVA) was also was employed to evaluate the significance of the laboratory data. For this purpose, Fracture energy until failure, total fracture energy, and $J_c$ were chosen as dependent variables and the temperature, fibre content and RAP content were chosen as the fixed factors.

## 4. Results and discussion

In this research, the GMDH and ANFIS models were applied on the fracture energy until failure, total fracture energy and the critical J integral of the asphalt mixtures containing different percentages of

**Table 6.** The results of the fracture tests.

| Run number | Sample Code | Factors evaluated: RAP Content (%) | Factors evaluated: Temperature (°C) | Factors evaluated: Fibre Content (%) | Response parameters: Fracture Energy (N.m) | Response parameters: Total Energy (N.m) | Response parameters: J integral (kj/m2) |
|---|---|---|---|---|---|---|---|
| 1 | 0% RAP + 0% Fibre + −15°C | 0 | −15 | 0 | 1.024 | 1.035 | 0.281 |
| 2 | 0% RAP + 0.06% Fibre + −15°C | 0 | −15 | 0.06 | 1.711 | 1.868 | 1.405 |
| 3 | 0% RAP + 0.12% Fibre + −15°C | 0 | −15 | 0.12 | 2.703 | 2.736 | 2.128 |
| 4 | 0% RAP + 0. 18% Fibre + −15°C | 0 | −15 | 0.18 | 1.108 | 1.131 | 0.397 |
| 5 | 0% RAP + 0% Fibre + 0°C | 0 | 0 | 0 | 3.669 | 4.111 | 3.026 |
| 6 | 0% RAP + 0.06% Fibre + 0°C | 0 | 0 | 0.06 | 5.566 | 6.912 | 4.415 |
| 7 | 0% RAP + 0.12% Fibre + 0°C | 0 | 0 | 0.12 | 7.542 | 8.941 | 6.867 |
| 8 | 0% RAP + 0.18% Fibre + 0°C | 0 | 0 | 0.18 | 4.762 | 5.515 | 4.679 |
| 9 | 0% RAP + 0% Fibre + 15°C | 0 | 15 | 0 | 2.874 | 15.150 | 2.612 |
| 10 | 0% RAP + 0.06% Fibre + 15°C | 0 | 15 | 0.06 | 4.312 | 27.937 | 3.857 |
| 11 | 0% RAP + 0.12% Fibre + 15°C | 0 | 15 | 0.12 | 3.627 | 39.392 | 3.320 |
| 12 | 0% RAP + 0. 18% Fibre + 15°C | 0 | 15 | 0.18 | 2.352 | 15.158 | 1.606 |
| 13 | 25% RAP + 0% Fibre + −15°C | 25 | −15 | 0 | 1.249 | 1.271 | 0.452 |
| 14 | 25% RAP + 0.06% Fibre + −15°C | 25 | −15 | 0.06 | 2.436 | 2.556 | 1.429 |
| 15 | 25% RAP + 0.12% Fibre + −15°C | 25 | −15 | 0.12 | 3.162 | 3.280 | 3.156 |
| 16 | 25% RAP + 0.18% Fibre + −15°C | 25 | −15 | 0.18 | 2.743 | 2.965 | 2.115 |
| 17 | 25% RAP + 0% Fibre + 0°C | 25 | 0 | 0 | 3.486 | 4.050 | 3.129 |
| 18 | 25% RAP + 0% Fibre + 0°C | 25 | 0 | 0.06 | 3.883 | 5.514 | 3.429 |
| 19 | 25% RAP + 0.12% Fibre + 0°C | 25 | 0 | 0.12 | 6.230 | 8.330 | 6.430 |
| 20 | 25% RAP + 0.18% Fibre + 0°C | 25 | 0 | 0.18 | 3.524 | 3.934 | 2.996 |
| 21 | 25% RAP + 0% Fibre + 15°C | 25 | 15 | 0 | 2.792 | 13.633 | 2.031 |
| 22 | 25% RAP + 0.06% Fibre + 15°C | 25 | 15 | 0.06 | 3.668 | 15.967 | 3.030 |
| 23 | 25% RAP + 0.12% Fibre + 15°C | 25 | 15 | 0.12 | 3.581 | 22.826 | 3.474 |
| 24 | 25% RAP + 0.18% Fibre + 15°C | 25 | 15 | 0.18 | 2.230 | 13.360 | 2.844 |
| 25 | 50% RAP + 0% Fibre + −15°C | 50 | −15 | 0 | 1.811 | 1.812 | 1.439 |
| 26 | 50% RAP + 0.06% Fibre + −15°C | 50 | −15 | 0.06 | 2.516 | 2.723 | 2.317 |
| 27 | 50% RAP + 0.12% Fibre + −15°C | 50 | −15 | 0.12 | 3.303 | 3.786 | 3.325 |
| 28 | 50% RAP + 0.18% Fibre + −15°C | 50 | −15 | 0.18 | 2.468 | 2.732 | 1.877 |
| 29 | 50% RAP + 0% Fibre + 0°C | 50 | 0 | 0 | 2.983 | 2.984 | 2.332 |
| 30 | 50% RAP + 0% Fibre + 0°C | 50 | 0 | 0.06 | 4.535 | 4.720 | 2.619 |
| 31 | 50% RAP + 0.12% Fibre + 0°C | 50 | 0 | 0.12 | 5.006 | 5.977 | 3.677 |
| 32 | 50% RAP + 0.18% Fibre + 0°C | 50 | 0 | 0.18 | 3.362 | 3.999 | 3.383 |
| 33 | 50% RAP + 0% Fibre + 15°C | 50 | 15 | 0 | 1.978 | 2.243 | 1.257 |
| 34 | 50% RAP + 0.06% Fibre + 15°C | 50 | 15 | 0.06 | 2.116 | 3.715 | 0.534 |
| 35 | 50% RAP + 0.12% Fibre + 15°C | 50 | 15 | 0.12 | 3.339 | 1.035 | 2.266 |
| 36 | 50% RAP + 0.18% Fibre + 15°C | 50 | 15 | 0.18 | 1.766 | 2.563 | 0.865 |
| 37 | 75% RAP + 0% Fibre + −15°C | 75 | −15 | 0 | 2.440 | 2.566 | 2.237 |
| 38 | 75% RAP + 0.06% Fibre + −15°C | 75 | −15 | 0.06 | 2.559 | 3.042 | 2.388 |
| 39 | 75% RAP + 0.12% Fibre + −15°C | 75 | −15 | 0.12 | 3.251 | 3.375 | 2.905 |
| 40 | 75% RAP + 0.18% Fibre + −15°C | 75 | −15 | 0.18 | 3.505 | 3.716 | 3.362 |
| 41 | 75% RAP + 0% Fibre + 0°C | 75 | 0 | 0 | 2.340 | 2.453 | 1.625 |
| 42 | 75% RAP + 0% Fibre + 0°C | 75 | 0 | 0.06 | 3.637 | 3.841 | 2.670 |
| 43 | 75% RAP + 0.12% Fibre + 0°C | 75 | 0 | 0.12 | 4.883 | 5.448 | 4.541 |
| 44 | 75% RAP + 0.18% Fibre + 0°C | 75 | 0 | 0.18 | 3.028 | 3.315 | 2.208 |
| 45 | 75% RAP + 0% Fibre + 15°C | 75 | 15 | 0 | 1.886 | 3.216 | 1.362 |
| 46 | 75% RAP + 0.06% Fibre + 15°C | 75 | 15 | 0.06 | 1.828 | 8.515 | 0.863 |
| 47 | 75% RAP + 0.12% Fibre + 15°C | 75 | 15 | 0.12 | 2.890 | 4.536 | 2.480 |
| 48 | 75% RAP + 0.18% Fibre + 15°C | 75 | 15 | 0.18 | 1.377 | 2.001 | 0.469 |
| 49 | 100% RAP + 0% Fibre + −15°C | 100 | −15 | 0 | 2.540 | 2.814 | 2.195 |
| 50 | 100% RAP + 0.06% Fibre + −15°C | 100 | −15 | 0.06 | 2.680 | 3.168 | 2.583 |
| 51 | 100% RAP + 0.12% Fibre + −15°C | 100 | −15 | 0.12 | 2.719 | 2.798 | 2.014 |
| 52 | 100% RAP + 0.18% Fibre + −15°C | 100 | −15 | 0.18 | 3.152 | 3.273 | 3.058 |
| 53 | 100% RAP + 0% Fibre + 0°C | 100 | 0 | 0 | 2.019 | 2.191 | 1.203 |
| 54 | 100% RAP + 0% Fibre + 0°C | 100 | 0 | 0.06 | 2.492 | 2.697 | 1.715 |
| 55 | 100% RAP + 0.12% Fibre + 0°C | 100 | 0 | 0.12 | 4.065 | 4.251 | 3.246 |
| 56 | 100% RAP + 0.18% Fibre + 0°C | 100 | 0 | 0.18 | 1.846 | 2.068 | 1.220 |
| 57 | 100% RAP + 0% Fibre + 15°C | 100 | 15 | 0 | 1.040 | 1.405 | 0.395 |
| 58 | 100% RAP + 0.06% Fibre + 15°C | 100 | 15 | 0.06 | 2.062 | 2.934 | 1.200 |
| 59 | 100% RAP + 0.12% Fibre + 15°C | 100 | 15 | 0.12 | 2.505 | 3.811 | 2.290 |
| 60 | 100% RAP + 0.18% Fibre + 15°C | 100 | 15 | 0.18 | 1.687 | 2.312 | 0.067 |

RAP and fibres at three temperatures of −15, 0 and 15°C. The total test results are presented in Table 6. It should be noted that all test results are the mean value of 4 replicates.

### 4.1. The effect of RAP material

The fracture test results at temperatures of −15, 0 and 15°C are presented in Figure 4. As can be seen in this Fig, the fracture energy until failure increases by increasing the RAP content at −15°C. The same trend is valid for the Jc test results. The reason is that in minus temperatures, asphalt materials are brittle, and fracture energy increases when brittle materials become stiffer. As adding RAP material stiffens the mixtures, the fracture energy and the Jc value increase by increasing the RAP content at minus temperatures. It should be noted that this trend is correct only for the load-related cracks, and as the cracking in the field occurs due to both loading and thermal stresses, the field performance may be different from the results of this section.

On the other hand, at intermediate temperatures of 0°C and 15°C, the fracture energy and the Jc values decrease by increasing the RAP content. This is mainly due to the decrease of the axial deformation in the fracture tests when the RAP content is raised. Overall, The RAP material has a positive effect on the fracture energy and Jc value of asphalt mixtures at minus temperatures, while it has a negative impact on fracture parameters at intermediate temperatures.

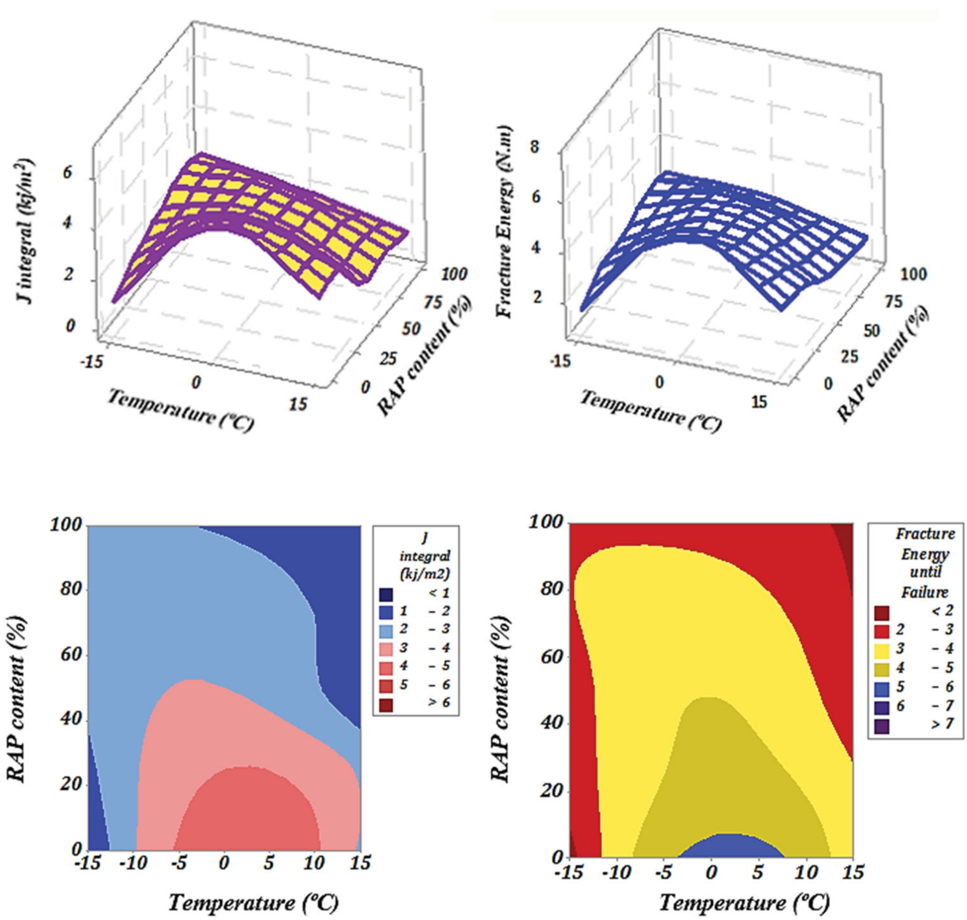


Colour online, B/W in print

**Figure 4.** The results of fracture energy and the $J_c$ value versus temperature and RAP content.

Colour online, B/W in print

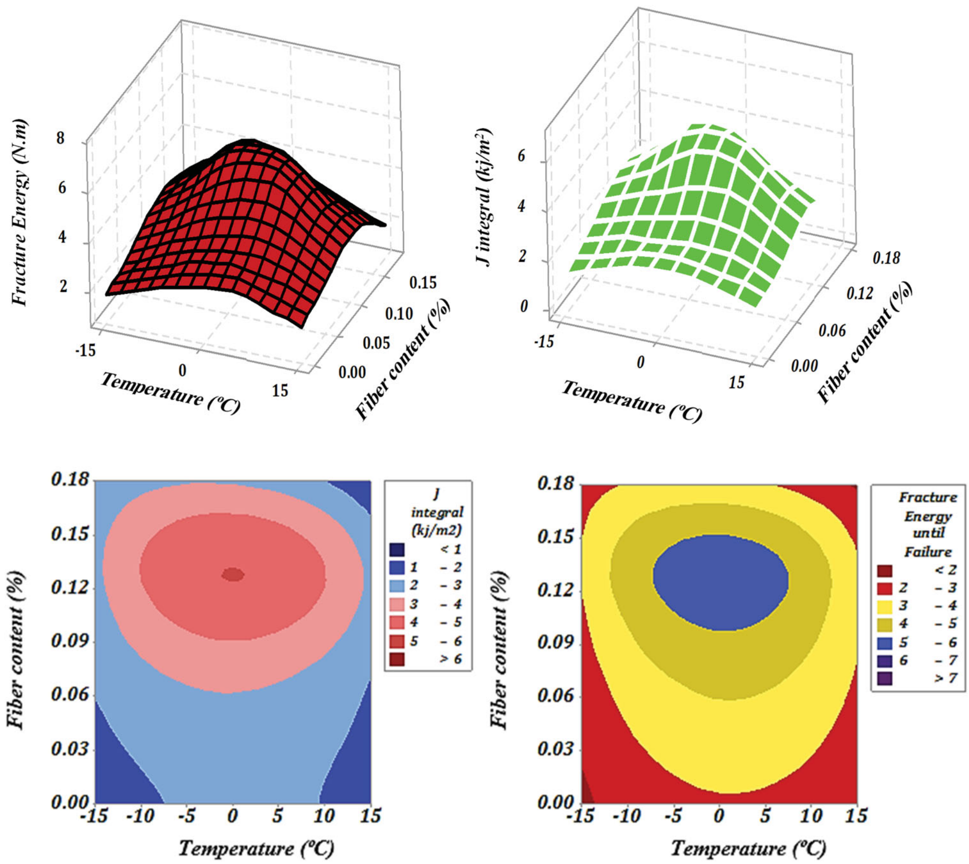


**Figure 5.** The results of fracture energy and the $J_C$ value versus temperature and fibre content.

## 4.2. The effect of fibres

The effect of glass fibre content on fracture energy and the Jc value of the mixtures at different temperatures are depicted in Figure 5. It can be seen that adding glass fibre substantially affects the fracture parameters of the mixtures, and both variables peak when the fibre content reaches to 0.12% especially at the temperature of 0°C.

## 4.3. Statistical analysis results

In this section, the analysis of variance (ANOVA) method has been performed to evaluate the significance of the effect of RAP, fibre, and temperature on the mechanical performance of fiber-reinforced high RAP asphalt mixtures. To analyze the ANOVA, firstly, the normal data were controlled using the Kolmogorov–Smirnov test and then the analysis was performed on normal data. Afterwards, in order to determine the effect of RAP and fibre on the performance of asphalt mixtures, the ANOVA analysis with a significance level of 95% had been performed using Minitab 17 software, and the results are presented in Table 7. According to the results of Fracture energy and J-integral, the *p*-value, which is meant to be less than 0.05 for 95% confidence, is lower than 0.05 when the RAP, fibre and temperature change, which means that the increase of RAP and fibre and temperature has a considerable effect on the significance level of 0.05 on fracture energy and J-integral parameter of asphalt mixture. However, the *P*-value of 0.160 indicates that the addition of fibres does not have a significant effect on the total fracture energy of the fiber-reinforced high RAP asphalt mixtures. Moreover, comparing the effect of

**Table 7.** ANOVA results for effect of RAP, fibre and temperature on physical properties of asphalt mixtures

| Source | Interval numbers | Type III Sum of Squares | Mean Square | F-Value | *p*-Value | Acceptance |
|---|---|---|---|---|---|---|
| **Fracture Energy** | | | | | | |
| RAP content | 0–100 (%) | 7.799 | 1.949 | 2.98 | 0.028 | Accept |
| Temperature | −15_+15 (°C) | 28.75 | 14.37 | 21.9 | 0.000 | Accept |
| Fibre content | 0–0.18 (%) | 23.04 | 7.682 | 11.7 | 0.000 | Accept |
| **Total Energy** | | | | | | |
| RAP content | 0–100 (%) | 603.8 | 150.9 | 5.43 | 0.001 | Accept |
| Temperature | −15_+15 (°C) | 598.5 | 299.2 | 10.7 | 0.000 | Accept |
| Fibre content | 0–0.18 (%) | 149.6 | 49.87 | 1.79 | 0.160 | Reject |
| **J integral** | | | | | | |
| RAP content | 0–100 (%) | 11.28 | 2.82 | 2.94 | 0.029 | Accept |
| Temperature | −15_+15 (°C) | 23.8 | 11.9 | 12.3 | 0.000 | Accept |
| Fibre content | 0–0.18 (%) | 26.29 | 8.762 | 9.12 | 0.000 | Accept |

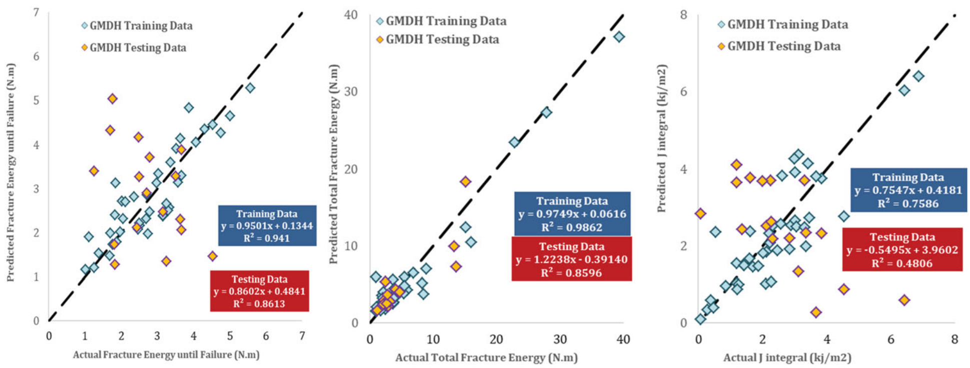


**Figure 6.** The Comparison between Predicted and experimental fracture parameters.

Colour online, B/W in print

each parameter shows that the temperature has the highest F-value and is the most influential parameter on the fracture performance of asphalt mixtures. Also, the comparison of the effect of fibres and RAP on the mechanical performance of asphalt mixtures shows that increasing the percentage of fibre with higher F-value has more influence than RAP on the fracture parameters of the studied mixtures.

## 4.4. The GMDH model

The GMDH model was fitted on the overall test results for predicting the parameters of fracture energy until failure, total fracture energy and Jc value in terms of temperature, RAP, and fibre content. A comparison of predicted and experimental fracture parameters is depicted in Figure 6. 80% of the data were used for training the model and 20% was used as testing data. It is seen that the training data fairly fit in the regression model models of fracture energy until failure and total fracture energy whereas the models are unable to predict some testing data. The GMDH model of the critical J integral value shows a small correlation with the actual data.

The statistical analysis of the regression models is also shown in Figure 7. It is seen from Figure 8 that a fair error and correlation exists in the results of the GMDH model, and the proposed GMDH model can fairly predict the experimental data of the SCB fracture tests. It can also be inferred from the data validation curves that the target and output curves match with each other in most cases. However, there are some points especially in the validation curves of J-integral that have large residuals and do not fit by the equations, which are highlighted in the graphs. These points have a strong adverse influence on the level of correlations and are shown in a normal probability plot of the regression prediction models.

Colour online, B/W in print

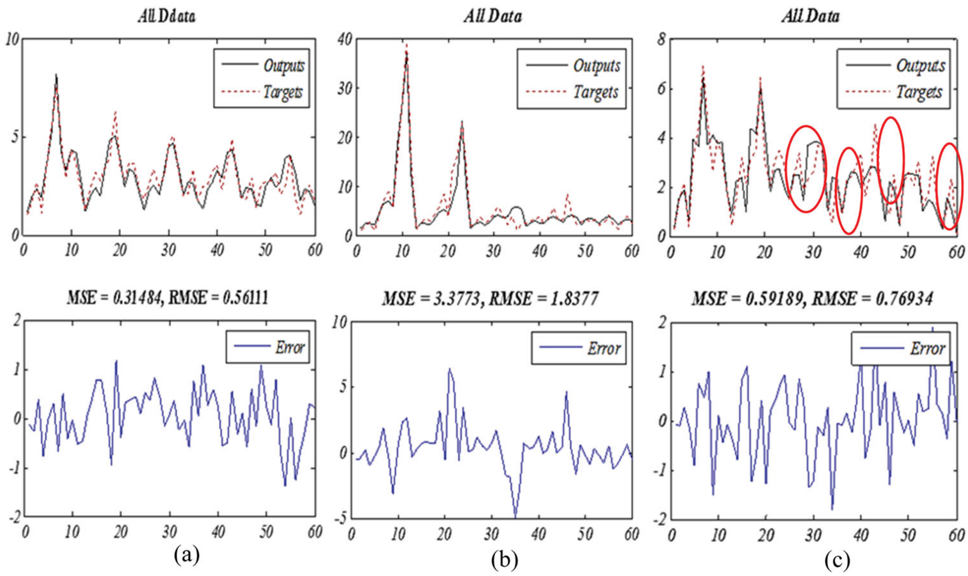


**Figure 7.** The data validation and the statistical parameters of the GMDH models: (a) Fracture energy until failure, (b) Total fracture energy, and (c) J-integral.

Colour online, B/W in print

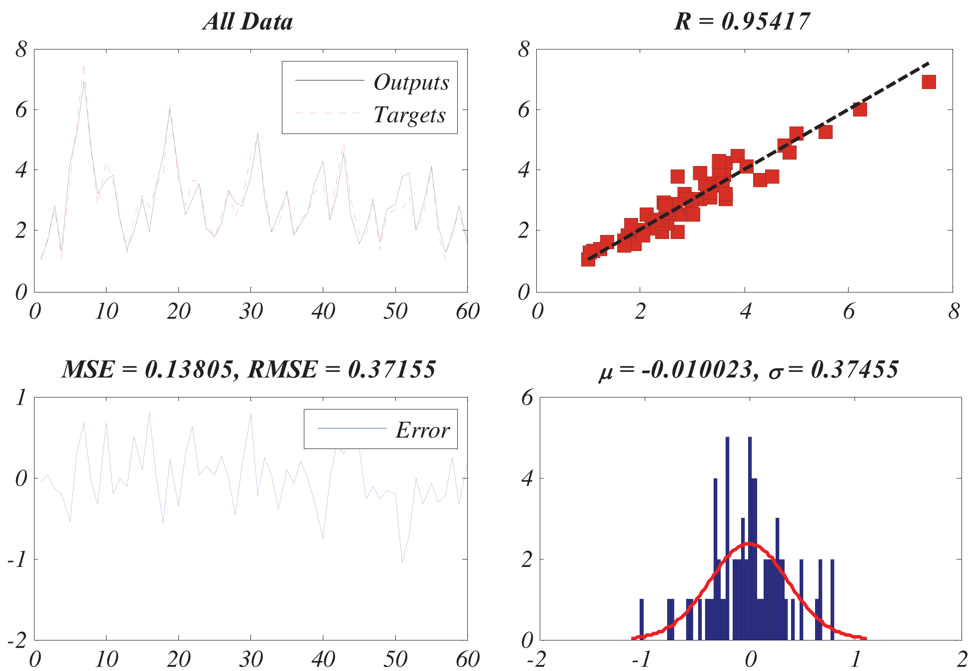


**Figure 8.** The statistical validation of the ANFIS model for the fracture energy until failure.

## 4.5. The ANFIS models

For designing the ANFIS models, at first, the model was run for different numbers of input membership functions and different algorithm membership functions to find the optimum neuro-fuzzy structure by comparing the statistical results of the model outputs. The results are listed in Table 8. It can be seen

**Table 8.** Details of the neuro-fuzzy structures.

| Neuro-Fuzzy Design | Inputs Variable: Temperature (°C) | Inputs Variable: Fibre Content (%) | Inputs Variable: RAP content (%) | Algorithm membership functions | Number of Epoch |
|---|---|---|---|---|---|
| | Number of membership function | | | | |
| Fracture energy until failure | 2 | 3 | 4 | gauss | 100 |
| Total fracture energy | 3 | 4 | 2 | gauss2 | 100 |
| J-integral | 2 | 4 | 3 | gauss2 | 100 |

**Table 9.** An instance of the details of the statistical analysis of different neuro-fuzzy structures of fracture energy until failure.

| Neuro-Fuzzy Design | Training data set: RMSE | COV | $R^2$ | Testing data set: RMSE | COV | $R^2$ | All data set: RMSE | VAF% | MAPE% | COV | $R^2$ |
|---|---|---|---|---|---|---|---|---|---|---|---|
| NFD-1 | 0.05161 | 10.349 | 0.65719 | 0.0624 | 12.39 | 0.3999 | 0.0551 | 72.0475 | 10.0088 | 11.01 | 0.5982 |
| NFD-2 | 0.01715 | 3.438 | 0.97025 | 0.6281 | 124.81 | 0.6707 | 0.3443 | 967.2253 | 14.4706 | 68.86 | 0.0918 |
| NFD-3 | 0.03562 | 7.143 | 0.85821 | 0.0482 | 9.57 | 0.6172 | 0.0398 | 85.3573 | 6.9277 | 7.96 | 0.8090 |
| NFD-4 | 0.02787 | 5.589 | 0.91777 | 0.0535 | 10.64 | 0.7035 | 0.0375 | 87.2440 | 5.7264 | 7.49 | 0.8582 |
| NFD-5 | 0.07679 | 15.400 | 0.24924 | 0.0821 | 16.31 | 0.1807 | 0.0784 | 43.4990 | 12.8396 | 15.68 | 0.0143 |
| NFD-6 | 0.02089 | 4.1902 | 0.95514 | 0.1422 | 28.25 | 0.1516 | 0.0798 | 41.4525 | 6.9292 | 15.96 | 0.5187 |
| NFD-7 | 0.06188 | 12.410 | 0.42045 | 0.0530 | 10.54 | 0.5870 | 0.0594 | 67.5538 | 10.0275 | 11.87 | 0.4884 |
| NFD-8 | 0.03908 | 7.837 | 0.82500 | 0.0373 | 7.41 | 0.8463 | 0.0385 | 86.3033 | 6.2663 | 7.70 | 0.8352 |
| NFD-9 | 0.07464 | 14.968 | 0.11442 | 0.0842 | 16.74 | 0.1756 | 0.0776 | 44.2615 | 13.0715 | 15.52 | 0.0489 |
| NFD-10 | 0.01891 | 3.793 | 0.96346 | 5.6690 | 1126.58 | 0.6744 | 3.1051 | 49.253 | 103.6582 | 621.0 | 0.1497 |
| NFD-11 | 0.05811 | 11.654 | 0.51893 | 0.0475 | 9.45 | 0.6767 | 0.0552 | 71.9259 | 9.5570 | 11.03 | 0.5788 |
| **NFD-12** | **0.02831** | **5.677** | **0.91502** | **0.0390** | **7.75** | **0.8327** | **0.0319** | **90.6202** | **5.4433** | **6.38** | **0.8936** |
| NFD-13 | 0.07465 | 14.972 | 0.11622 | 0.0814 | 16.18 | 0.1391 | 0.0767 | 45.5148 | 12.9459 | 15.34 | 0.0243 |
| NFD-14 | 0.01622 | 3.252 | 0.97332 | 5.7541 | 1143.48 | 0.6656 | 3.1517 | 89624.8 | 95.7819 | 630.33 | 0.1477 |
| NFD-15 | 0.05738 | 11.507 | 0.53535 | 0.0559 | 11.11 | 0.5906 | 0.0569 | 70.0047 | 10.0449 | 11.38 | 0.5666 |
| NFD-16 | 0.02424 | 4.8615 | 0.93894 | 0.0595 | 11.81 | 0.6052 | 0.0384 | 86.7462 | 5.7819 | 7.67 | 0.8503 |
| NFD-17 | 0.07442 | 14.925 | 0.10310 | 0.0862 | 17.13 | 0.1353 | 0.0781 | 43.5000 | 13.2434 | 15.62 | 0.0382 |
| NFD-18 | 0.02062 | 4.135 | 0.95633 | 0.2910 | 57.82 | 0.1244 | 0.1603 | 137.2851 | 10.8434 | 32.05 | 0.0198 |
| NFD-19 | 0.05751 | 11.533 | 0.53254 | 0.0503 | 9.99 | 0.6149 | 0.0554 | 71.5864 | 9.7951 | 11.08 | 0.5688 |
| NFD-20 | 0.02523 | 5.060 | 0.93349 | 0.0620 | 12.32 | 0.6029 | 0.0400 | 85.6026 | 5.8648 | 7.99 | 0.8411 |

that the neuro-fuzzy structure containing two, three and four membership functions of temperature, fibre content and RAP content respectively with a gauss algorithm had the best statistical correlation and was chosen as the optimum neuro-fuzzy structure for fracture energy until failure. The optimum neuro-fuzzy structure of the total fracture energy and j-integral models are also shown in Table 8. Moreover, an instance of the details of the statistical analysis of different neuro-fuzzy structures of fracture energy until failure is provided in Table 9.

The level of correlation and the statistical validation of the ANFIS models developed for the fracture energy until failure, total fracture energy, and J-integral are calculated and shown in Figures 8–10. As can be seen in these Figures, the proposed ANFIS models for all fracture parameters have a strong correlation with the experimental results. It can be inferred from the provided statistical details that the highest level of correlation is related to the model of total fracture energy, and the models of fracture energy until failure and J-integral are in the next ranks.

### *4.6. The comparison between the GMDH and ANFIS models*

The comparison between the GMDH and ANFIS models is presented in Figure 11. As shown, the ANFIS method performs more accurately than the GMDH method in modelling the experimental fracture

Colour online, B/W in print

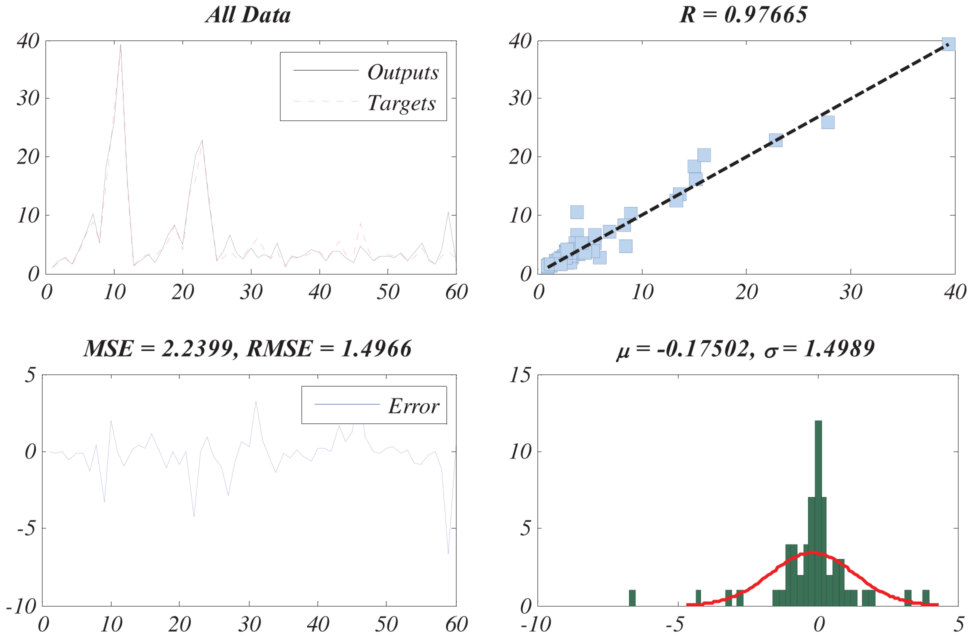


**Figure 9.** The statistical validation of the ANFIS model for the total fracture energy.

Colour online, B/W in print

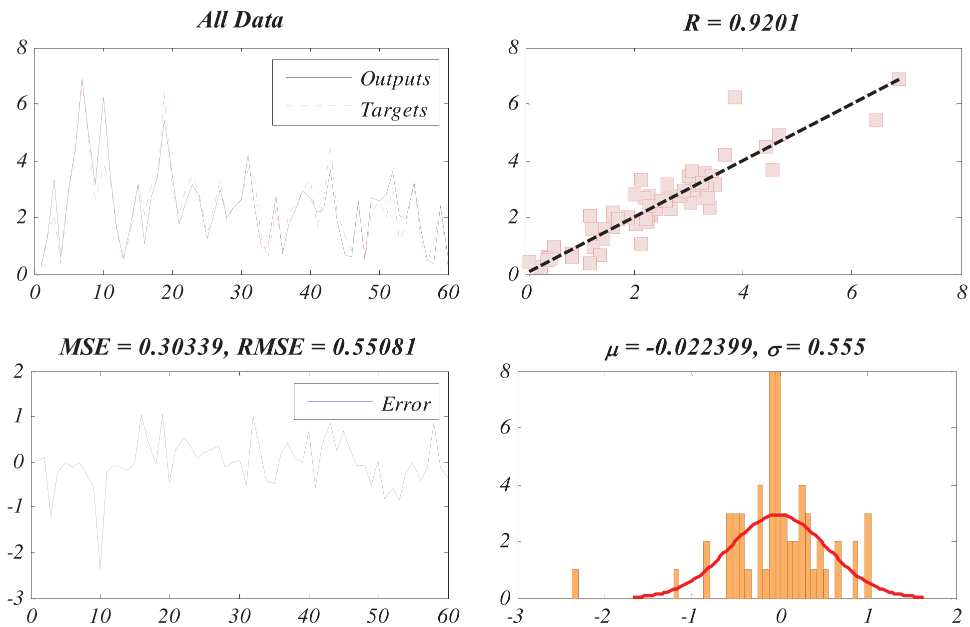


**Figure 10.** The statistical validation of the ANFIS model for the $J_c$ value.

parameters, and all statistical parameters are better for the ANFIS models for all investigated fracture parameters. The GMDH model performed poorly in predicting the J-integral experimental data. However, it had a fair correlation with the experimental data of fracture energy until failure and total fracture energy.

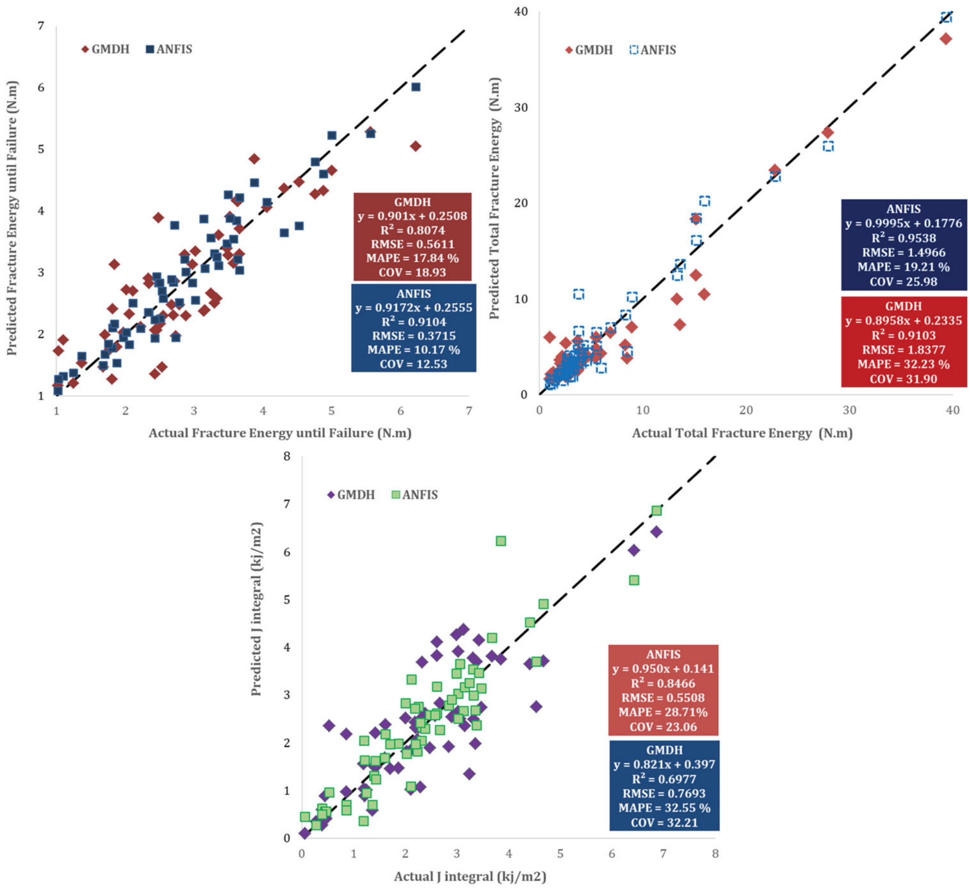


**Figure 11.** The comparison between the GMDH and ANFIS models.

Colour online, B/W in print

## 5. Conclusion

In this research, the effectiveness of the GMDH and the ANFIS modelling methods on predicting the fracture parameters of asphalt mixtures was investigated. For this purpose, the SCB fracture tests were conducted on the asphalt mixtures containing different percentages of RAP material and glass fibre at three different temperatures of −15, 0 and 15°C, and the fracture energy until failure, total fracture energy, and the critical J-integral value were modelled using the GMDH and ANFIS methods. The results indicated that the ANFIS method was more promising than the GMDH method in predicting the fracture parameters of the studied asphalt mixtures. Other conclusions can be drawn as follows:

- At negative temperatures, the RAP material had a positive impact on the fracture energy and the Jc value of asphalt mixtures, and the fracture parameters improved by increasing the RAP content. However, the opposite occurred at temperatures of 0°C and 15°C, and adding RAP material resulted in a reduction in fracture energy and Jc at these temperatures. Glass fibres have a positive effect on the fracture performance of the recycled mixtures at all temperatures and can be used as an alternative to compensate for the negative impact of the RAP material. However, the results of this study may differ from the actual cracking performance of asphalt mixtures as only the load-related cracking performance is investigated in this research and the effect of thermal stresses is not considered. Therefore, it is recommended to consider the effect of thermal stresses and compare it with the results of this research in future studies.

- The ANFIS method successfully modelled all fracture parameters in terms of temperature, fibre content and RAP content with a high level of correlation.
- The GMDH model was unable to predict the J-integral data. However, it had a fair correlation with the experimental data of the fracture energy until failure and total fracture energy.

## ORCID

*Ali Moniri* http://orcid.org/0000-0002-7416-1312

## References

Abraham, A. (2005). Adaptation of fuzzy inference system using neural learning. In *Fuzzy systems engineering* (pp. 53–83). Springer.https://doi.org/10.1007/11339366_3.

Abtahi, S. M., Sheikhzadeh, M., & Hejazi, S. M. (2010). Fiber-reinforced asphalt-concrete – A review. *Construction and Building Materials*, *24*(6), 871–877. https://doi.org/10.1016/j.conbuildmat.2009.11.009

A. D. T245. (2004). *Standard method of test for resistance to plastic flow of bituminous mixtures using Marshall Apparatus*. ed: AASHTO Washington, DC.

Aliha, M. (2019). On predicting mode II fracture toughness (KIIc) of hot mix asphalt mixtures using the strain energy density criterion. *Theoretical and Applied Fracture Mechanics*, *99*, 36–43. https://doi.org/10.1016/j.tafmec.2018.11.001

Aliha, M. R. M., Bahmani, A., & Akhondi, S. (2016). A novel test specimen for investigating the mixed mode I+III fracture toughness of hot mix asphalt composites – experimental and theoretical study. *International Journal of Solids and Structures*, *90*, 167–177. https://doi.org/10.1016/j.ijsolstr.2016.03.018

Aliha, M. R. M., Behbahani, H., Fazaeli, H., & Rezaifar, M. H. (2014). Study of characteristic specification on mixed mode fracture toughness of asphalt mixtures. *Construction and Building Materials*, *54*, 623–635. https://doi.org/10.1016/j.conbuildmat.2013.12.097

Aliha, M., Fazaeli, H., Aghajani, S., & Nejad, F. M. (2015). Effect of temperature and air void on mixed mode fracture toughness of modified asphalt mixtures. *Construction and Building Materials*, *95*, 545–555. https://doi.org/10.1016/j.conbuildmat.2015.07.165

Aliha, M., & Sarbijan, M. (2016). Effects of loading, geometry and material properties on fracture parameters of a pavement containing top-down and bottom-up cracks. *Engineering Fracture Mechanics*, *166*, 182–197. https://doi.org/10.1016/j.engfracmech.2016.08.028

Aliha, M., Sarbijan, M., & Bahmani, A. (2017). Fracture toughness determination of modified HMA mixtures with two novel disc shape configurations. *Construction and Building Materials*, *155*, 789–799. https://doi.org/10.1016/j.conbuildmat.2017.08.093

Ameri, M., Mansourkhaki, A., & Daryaee, D. (2019). Evaluation of fatigue behavior of asphalt binders containing reclaimed asphalt binder using simplified viscoelastic continuum damage approach. *Construction and Building Materials*, *202*, 374–386. https://doi.org/10.1016/j.conbuildmat.2019.01.021

Ameri, M., Nowbakht, S., Molayem, M., & Aliha, M. (2016). Investigation of fatigue and fracture properties of asphalt mixtures modified with carbon nanotubes. *Fatigue & Fracture of Engineering Materials & Structures*, *39*(7), 896–906. https://doi.org/10.1111/ffe.12408

Ayazi, M. J., Moniri, A., & Barghabany, P. (2017). Moisture susceptibility of warm mixed-reclaimed asphalt pavement containing Sasobit and Zycotherm additives. *Petroleum Science and Technology*, *35*(9), 890–895. https://doi.org/10.1080/10916466.2017.1290655

Behbahani, H., Aliha, M., Reza, M., Fazaeli, H., & Aghajani, S. (2013). Experimental fracture toughness study for some modified asphalt mixtures. *Advanced Materials Research*, Trans Tech Publ, *723*, 337–344. https://doi.org/10.4028/www.scientific.net/AMR.723.337

Behbahani, H., Ayazi, M. J., & Moniri, A. (2017). Laboratory investigation of rutting performance of warm mix asphalt containing high content of reclaimed asphalt pavement. *Petroleum Science and Technology*, *35*(15), 1556–1561. https://doi.org/10.1080/10916466.2017.1316738

Dehghan, Z., & Modarres, A. (2017). Evaluating the fatigue properties of hot mix asphalt reinforced by recycled PET fibers using 4-point bending test. *Construction and Building Materials*, *139*, 384–393. https://doi.org/10.1016/j.conbuildmat.2017.02.082

Ding, X., Chen, L., Ma, T., Ma, H., Gu, L., Chen, T., & Ma, Y. (2019). Laboratory investigation of the recycled asphalt concrete with stable crumb rubber asphalt binder. *Construction and Building Materials*, *203*, 552–557. https://doi.org/10.1016/j.conbuildmat.2019.01.114

Enieb, M., Diab, A., & Yang, X. (2019). Short-and long-term properties of glass fiber reinforced asphalt mixtures. *International Journal of Pavement Engineering*, 1–13. https://doi.org/10.1080/10298436.2019.1577421

Fattahi Amirdehi, H. R., Aliha, M. R. M., Moniri, A., & Torabi, A. R. (2019). Using the generalized maximum tangential stress criterion to predict mode II fracture of hot mix asphalt in terms of mode I results – A statistical analysis. *Construction and Building Materials*, *213*, 483–491. https://doi.org/10.1016/j.conbuildmat.2019.04.067

Haghighat Pour, P. J., Aliha, M. R. M., & Keymanesh, M. R. (2018). Evaluating mode I fracture resistance in asphalt mixtures using edge notched disc bend ENDB specimen with different geometrical and environmental conditions. *Engineering Fracture Mechanics*, *190*, 245–258. https://doi.org/10.1016/j.engfracmech.2017.11.007

Haghshenas, H., Nabizadeh, H., Kim, Y.-R., & Santosh, K. (2016). *Research on high-rap asphalt mixtures with rejuvenators and WMA additives*.

Ivakhnenko, A. G. (1971). Polynomial theory of complex systems. *IEEE Transactions on Systems, Man, and Cybernetics*, *4*(4), 364–378. https://doi.org/10.1109/TSMC.1971.4308320

Jahanbakhsh, H., Hosseini, P., Nejad, F. M., & Habibi, M. (2019). Intermediate temperature fracture resistance evaluation of cement emulsified asphalt mortar. *Construction and Building Materials*, *197*, 1–11. https://doi.org/10.1016/j.conbuildmat.2018.11.170

Jing, R., Varveri, A., Liu, X., Scarpas, A., & Erkens, S. (2019). Laboratory and field Aging effect on bitumen Chemistry and Rheology in Porous asphalt mixture. *Transportation Research Record*, *2673*(3). https://doi.org/10.1177/0361198119833362.

Khanghahi, S. H., & Tortum, A. (2018). Determination of the optimum Conditions for Gilsonite and glass Fiber in HMA under mixed mode I/III loading in fracture tests. *Journal of Materials in Civil Engineering*, *30*(7), 04018130. https://doi.org/10.1061/(ASCE)MT.1943-5533.0002278

Kim, Y., Mallick, R., Bhowmick, S., & Chen, B.-L. (2013). Nonlinear system identification of large-scale smart pavement systems. *Expert Systems with Applications*, *40*(9), 3551–3560. https://doi.org/10.1016/j.eswa.2012.12.062

Kodippily, S., Holleran, G., & Henning, T. F. (2017). Deformation and cracking performance of recycled asphalt paving mixes containing polymer-modified binder. *Road Materials and Pavement Design*, *18*(2), 425–439. https://doi.org/10.1080/14680629.2016.1181559

Kök, B. V., Yilmaz, M., Çakiroğlu, M., Kuloğlu, N., & Şengür, A. (2013). Neural network modeling of SBS modified bitumen produced with different methods. *Fuel*, *106*, 265–270. https://doi.org/10.1016/j.fuel.2012.12.073

Korayem, A. H., Ziari, H., Hajiloo, M., & Moniri, A. (2018). Rutting and fatigue performance of asphalt mixtures containing amorphous carbon as filler and binder modifier. *Construction and Building Materials*, *188*, 905–914. https://doi.org/10.1016/j.conbuildmat.2018.08.179

Ling, M., Luo, X., Chen, Y., Hu, S., & Lytton, R. L. (2019). A calibrated mechanics-based model for top-down cracking of asphalt pavements. *Construction and Building Materials*, *208*, 102–112. https://doi.org/10.1016/j.conbuildmat.2019.02.090

Luo, X., Zhang, Y., & Lytton, R. L. (2016). Implementation of pseudo J-integral based Paris' law for fatigue cracking in asphalt mixtures and pavements. *Materials and Structures*, *49*(9), 3713–3732. https://doi.org/10.1617/s11527-015-0750-z

Mansourian, A., Razmi, A., & Razavi, M. (2016). Evaluation of fracture resistance of warm mix asphalt containing jute fibers. *Construction and Building Materials*, *117*, 37–46. https://doi.org/10.1016/j.conbuildmat.2016.04.128

Mansourkhaki, A., Ameri, M., & Daryaee, D. (2019a). Application of different modifiers for improvement of chemical characterization and physical-rheological parameters of reclaimed asphalt binder. *Construction and Building Materials*, *203*, 83–94. https://doi.org/10.1016/j.conbuildmat.2019.01.086

Mansourkhaki, A., Ameri, M., Habibpour, M., & Shane Underwood, B. (2020a). Chemical Composition and Rheological characteristics of binders containing RAP and rejuvenator. *Journal of Materials in Civil Engineering*, *32*(4), 04020026. https://doi.org/10.1061/(ASCE)MT.1943-5533.0003016

Mansourkhaki, A., Ameri, M., Habibpour, M., & Underwood, B. S. (2019b). *Fractional Composition and High Temperature Rheological Properties of Modified RAP Binder*.

Mansourkhaki, A., Ameri, M., Habibpour, M., & Underwood, B. S. (2020b). Relations between colloidal indices and low-temperature properties of reclaimed binder modified with softer binder, oil-rejuvenator and polybutadiene rubber. *Construction and Building Materials*, *239*, 117800. https://doi.org/10.1016/j.conbuildmat.2019.117800

McDaniel, R. S. (2015). *Fiber additives in asphalt mixtures* (no. Project 20-05 (Topic 45-15)).

Minhajuddin, M., Saha, G., & Biligiri, K. P. (2015). Crack propagation parametric assessment of modified asphalt mixtures using linear elastic fracture mechanics approach. *Journal of Testing and Evaluation*, *44*(1), 471–483. https://doi.org/10.1520/JTE20140510.

Moghaddam, T. B., & Baaj, H. (2016). The use of rejuvenating agents in production of recycled hot mix asphalt: A systematic review. *Construction and Building Materials*, *114*, 805–816. https://doi.org/10.1016/j.conbuildmat.2016.04.015

Moghaddam, T. B., Soltani, M., Karim, M. R., Shamshirband, S., Petković, D., & Baaj, H. (2015). Estimation of the rutting performance of polyethylene terephthalate modified asphalt mixtures by adaptive neuro-fuzzy methodology. *Construction and Building Materials*, *96*, 550–555. https://doi.org/10.1016/j.conbuildmat.2015.08.043

Mohammad, L. N., Kim, M., & Elseifi, M. (2012). *Characterization of asphalt mixture's fracture resistance using the semi-circular bending (SCB) test*. 7th RILEM international conference on cracking in pavements, Springer, pp. 1-10, https://doi.org/10.1007/978-94-007-4566-7_1.

Mohandes, M., Rehman, S., & Rahman, S. (2011). Estimation of wind speed profile using adaptive neuro-fuzzy inference system (ANFIS). *Applied Energy*, *88*(11), 4024–4032. https://doi.org/10.1016/j.apenergy.2011.04.015

Moniri, A., Ziari, H., Aliha, M., & Saghafi, Y. (2019). Laboratory study of the effect of oil-based recycling agents on high RAP asphalt mixtures. *International Journal of Pavement Engineering*, 1–12. https://doi.org/10.1080/10298436.2019.1696461

Morea, F., & Zerbino, R. (2018). Improvement of asphalt mixture performance with glass macro-fibers. *Construction and Building Materials*, *164*, 113–120. https://doi.org/10.1016/j.conbuildmat.2017.12.198

Naderi, K., Nakhaei, M., Jalali, F., Nasrekani, A. A., & Timm, D. H. (2019). *Low PG Determination of Neat Binders: A Comparison Between AASHTO Procedure and Time Temperature Superposition Approach*.

Najd, A., Chao, Z., & Ying, G. (2005). Experiments of fracture behavior of glass fiber reinforced asphalt concrete. *Journal of Chang'an University (Natural Science Edition)*, *25*(3).

Park, P., El-Tawil, S., Park, S.-Y., & Naaman, A. E. (2015). Cracking resistance of fiber reinforced asphalt concrete at −20°C. *Construction and Building Materials*, *81*, 47–57. https://doi.org/10.1016/j.conbuildmat.2015.02.005

Pourtahmasb, M. S., Karim, M. R., & Shamshirband, S. (2015). Resilient modulus prediction of asphalt mixtures containing recycled Concrete aggregate using an adaptive neuro-fuzzy methodology. *Construction and Building Materials*, *82*, 257–263. https://doi.org/10.1016/j.conbuildmat.2015.02.030

Qin, X., Shen, A., Guo, Y., Li, Z., & Lv, Z. (2018). Characterization of asphalt mastics reinforced with basalt fibers. *Construction and Building Materials*, *159*, 508–516. https://doi.org/10.1016/j.conbuildmat.2017.11.012

Sabouri, M., Mirzaiyan, D., & Moniri, A. (2018). Effectiveness of linear Amplitude Sweep (LAS) asphalt binder test in predicting asphalt mixtures fatigue performance. *Construction and Building Materials*, *171*, 281–290. https://doi.org/10.1016/j.conbuildmat.2018.03.146

Saha, G., & Biligiri, K. P. (2015). Fracture damage evaluation of asphalt mixtures using Semi-Circular Bending test based on fracture energy approach. *Engineering Fracture Mechanics*, *142*, 154–169. https://doi.org/10.1016/j.engfracmech.2015.06.009

Saha, G., & Biligiri, K. P. (2016). Fracture properties of asphalt mixtures using semi-circular bending test: A state-of-the-art review and future research. *Construction and Building Materials*, *105*, 103–112. https://doi.org/10.1016/j.conbuildmat.2015.12.046

Sezavar, R., Shafabakhsh, G., & Mirabdolazimi, S. M. (2019). New model of moisture susceptibility of nano silica-modified asphalt concrete using GMDH algorithm. *Construction and Building Materials*, *211*, 528–538. https://doi.org/10.1016/j.conbuildmat.2019.03.114

Sharifi, E., Sadjadi, S. J., Aliha, M., & Moniri, A. (2020). Optimization of high-strength self-consolidating concrete mix design using an improved Taguchi optimization method. *Construction and Building Materials*, *236*, 117547. https://doi.org/10.1016/j.conbuildmat.2019.117547

Sirin, O., Paul, D. K., & Kassem, E. (2018). State of the art study on aging of asphalt mixtures and use of antioxidant additives. *Advances in Civil Engineering*, *2018*. https://doi.org/10.1155/2018/3428961

Slebi-Acevedo, C. J., Lastra-González, P., Pascual-Muñoz, P., & Castro-Fresno, D. (2019). Mechanical performance of fibers in hot mix asphalt: A review. *Construction and Building Materials*, *200*, 756–769. https://doi.org/10.1016/j.conbuildmat.2018.12.171

Song, W., Huang, B., & Shu, X. (2018). Influence of warm-mix asphalt technology and rejuvenator on performance of asphalt mixtures containing 50% reclaimed asphalt pavement. *Journal of Cleaner Production*, *192*, 191–198. https://doi.org/10.1016/j.jclepro.2018.04.269

Tabatabaei, S. A., Khaledi, S., & Jahantabi, A. (2013). Modeling the deduct value of the pavement condition of asphalt pavement by adaptive neuro fuzzy inference system. *International Journal of Pavement Research and Technology*, *6*(1), 59–65.

Zaumanis, M., & Mallick, R. B. (2015). Review of very high-content reclaimed asphalt use in plant-produced pavements: State of the art. *International Journal of Pavement Engineering*, *16*(1), 39–55. https://doi.org/10.1080/10298436.2014.893331

Zaumanis, M., Mallick, R. B., & Frank, R. (2014). Determining optimum rejuvenator dose for asphalt recycling based on Superpave performance grade specifications. *Construction and Building Materials*, *69*, 159–166. https://doi.org/10.1016/j.conbuildmat.2014.07.035

Zaumanis, M., Mallick, R. B., & Frank, R. (2015). Evaluation of different recycling agents for restoring aged asphalt binder and performance of 100% recycled asphalt. *Materials and Structures*, *48*(8), 2475–2488. https://doi.org/10.1617/s11527-014-0332-5

Zhou, Z., Gu, X., Dong, Q., Ni, F., & Jiang, Y. (2019). Rutting and fatigue cracking performance of SBS-RAP blended binders with a rejuvenator. *Construction and Building Materials*, *203*, 294–303. https://doi.org/10.1016/j.conbuildmat.2019.01.119

Zhou, Z., Gu, X., Li, Q., Ni, F., & Yuan, R. (2016). Use of rejuvenator, styrene-butadiene rubber latex, and warm-mix asphalt technology to achieve conventional mixture performance with 50% reclaimed asphalt pavement. *Transportation Research Record: Journal of the Transportation Research Board*, *2575*(1), 160–167. https://doi.org/10.3141/2575-17

Ziari, H., Aliha, M., Moniri, A., & Saghafi, Y. (2020). Crack resistance of hot mix asphalt containing different percentages of reclaimed asphalt pavement and glass fiber. *Construction and Building Materials*, *230*, 117015. https://doi.org/10.1016/j.conbuildmat.2019.117015

Ziari, H., Amini, A., Goli, A., & Mirzaeiyan, D. (2018). Predicting rutting performance of carbon nano tube (CNT) asphalt binders using regression models and neural networks. *Construction and Building Materials*, *160*, 415–426. https://doi.org/10.1016/j.conbuildmat.2017.11.071

Ziari, H., & Moniri, A. (2019). Laboratory evaluation of the effect of synthetic Polyolefin-glass fibers on performance properties of hot mix asphalt. *Construction and Building Materials*, *213*, 459–468. https://doi.org/10.1016/j.conbuildmat.2019.04.084

Ziari, H., Moniri, A., Ayazi, M. J., & Nakhaei, M. (2016d). Investigation of rutting performance of wma mixtures containing copper slag. *International Journal of Transportation Engineering*, *3*(3), 227–235. https://doi.org/10.22119/ijte.2016.14775.

Ziari, H., Moniri, A., Bahri, P., & Saghafi, Y. (2019a). The effect of rejuvenators on the aging resistance of recycled asphalt mixtures. *Construction and Building Materials*, *224*, 89–98. https://doi.org/10.1016/j.conbuildmat.2019.06.181

Ziari, H., Moniri, A., Bahri, P., & Saghafi, Y. (2019b). Evaluation of performance properties of 50% recycled asphalt mixtures using three types of rejuvenators. *Petroleum Science and Technology*, 1–7. https://doi.org/10.1080/10916466.2018.1550505.

Ziari, H., Moniri, A., Imaninasab, R., & Nakhaei, M. (2017). Effect of copper slag on performance of warm mix asphalt. *International Journal of Pavement Engineering*, 1–7.

Ziari, H., Moniri, A., & Norouzi, N. (2019). The effect of nanoclay as bitumen modifier on rutting performance of asphalt mixtures containing high content of rejuvenated reclaimed asphalt pavement. *Petroleum Science and Technology*, 1–6. https://doi.org/10.1080/10916466.2018.1471489.

Ziari, H., Nakhaei, M., Akbari Nasrekani, A., & Moniri, A. (2016b). Characterization of rutting resistance of EBS-modified asphalt mixtures. *Petroleum Science and Technology*, *34*(13), 1107–1112. https://doi.org/10.1080/10916466.2016.1181655

Ziari, H., Saghafi, Y., Moniri, A., & Bahri, P. (2019c). The effect of polyolefin-aramid fibers on performance of hot mix asphalt. *Petroleum Science and Technology*, 1–7. https://doi.org/10.1080/10916466.2019.1697286.

Ziari, H., Sobhani, J., Ayoubinejad, J., & Hartmann, T. (2016a). Analysing the accuracy of pavement performance models in the short and long terms: GMDH and ANFIS methods. *Road Materials and Pavement Design*, *17*(3), 619–637. https://doi.org/10.1080/14680629.2015.1108218

Ziari, H., Sobhani, J., Ayoubinejad, J., & Hartmann, T. (2016c). Prediction of IRI in short and long terms for flexible pavements: ANN and GMDH methods. *International Journal of Pavement Engineering*, *17*(9), 776–788. https://doi.org/10.1080/10298436.2015.1019498